Frontiers in Mechanochemistry and Mechanical Alloying

INCOME2008
1-4 December, 2008

COMPOSITION DEPENDENT PROPERTIES OF MECHANICALLY ALLOYED AMORPHOUS Fe-Zr-B POWDERS

Debabrata Mishra[ξ], A. Perumal, A. Srinivasan
Department of Physics, Indian Institute of Technology Guwahati, Guwahati - 781039, India

Keywords: Mechanical alloying, Crystallization temperature, Coercivity, Anisotropy

Abstract

We report the preparation of Fe-Zr-B amorphous alloys by mechanical alloying in a planetary ball mill for 100 hours. Structural investigation of the as-milled powders has been carried out using X-ray diffraction, transmission electron microscope and scanning electron microscope techniques. The crystallization behavior of the amorphous powders has been studied using a differential scanning calorimeter. Magnetic properties of the powders have been investigated using a vibrating sample magnetometer. It has been observed that both thermal and magnetic properties of the as-milled alloy powders vary up to a critical boron concentration of 7.5 at.%. The coercivity of the amorphous powders was compared to that of melt spun ribbons. The high coercivity of the as milled alloy powder has been attributed to the effective anisotropy of the as-milled powders.

Introduction

Amorphous metallic alloys have drawn a lot of interest over the last few decades due to their high strength, good ductility, high fracture toughness, good corrosion resistance and desirable soft magnetic properties [1,2]. Because of these properties, metallic glasses have found several large scale industrial applications. Amorphous alloys or metallic glasses can be prepared by different processing techniques such as melt quenching, sputter deposition, plasma processing, laser processing, mechanical alloying etc. Amorphization by mechanical alloying (MA) process is a successful technique for preparing large scale material [3]. It needs less expensive equipment, room temperature processing condition and more importantly high quenching rate is not needed as in the case of melt spun technique to produce amorphous alloys. In the MA process, a blend of elemental or alloy powders is subjected to highly energetic compressive impact forces in a ball-mill. These impact forces result in repeated cold welding and fracture of the powder particles. During the early stages, ball milling produces powder particles with a characteristically layered microstructure due to cold welding and repeated mechanical deformation [4,5,6]. Further milling leads to an ultrafine composite or solid solution of the elemental powders and finally a homogeneous amorphous alloy is formed by solid-state inter diffusion reaction. The heavy plastic deformation generates a large number of point defects, which at low temperature can modify not only the diffusion behavior but also the chemical order of the crystalline structure [7].

Amorphous Fe-Zr-B alloys show interesting low temperature properties as well as ultra low coercivities [8, 9]. It has been reported [10] that mechanically alloyed Fe-Zr binary alloys have an amorphous state in the composition range of 22 to 70 at%. Zr and supersaturated bcc Fe solid solution is formed for Zr addition up to 5 at.%. In the present study we have prepared amorphous $Fe_{65-x}Zr_{35}B_x$ (x=2.5, 5, 7.5, 10) powder by MA method. The thermal and magnetic properties of the amorphous powders are presented in this paper.

Experimental Details

Weighed quantities of elemental Fe, Zr and B (purity of 99.9 %) powders corresponding to compositions of $Fe_{100-x}Zr_{35}B_x$ (x=2.5, 5, 7.5, 10) were sealed in a hardened steel vial filled with high purity argon gas. MA of the powder mixture was performed in an Insmart planetary ball mill operated at 500 rpm. Hardened steel balls of 8 mm diameter were used and the ball to powder weight ratio was maintained at 20:1. In order to avoid excessive heating, the mill was programmed to halt for 10 minutes after every 15 minutes of operation. All the powder compositions were milled for 100 hours, where most of the investigated samples attained the amorphous state. The crystal structure of the as-milled powders was characterized using X-ray diffractometer (Seifert 3003, T/T). The microstructure of the powders was analyzed using Scanning Electron Microscope (SEM, Leo 1430 VP) and Transmission Electron Microscope (TEM, JEOL 2100). The compositions of the powders were determined by Energy Dispersive Spectroscopy (EDS) unit attached to the SEM. Thermal analysis of the as-milled powders was carried out using a Differential Scanning Calorimeter (DSC 7, Perkin-Elmer) operated under different constant heating rates of 15, 20, 25 and 30 K/min under dry nitrogen gas atmosphere. Room temperature magnetic properties of the as-milled powders were measured using a Vibrating Sample Magnetometer (VSM, Lakeshore Model 7410) in applied field range of ± 2 Tesla.

Results and Discussions

Figure 1 shows the X-ray diffraction (XRD) pattern of amorphous $Fe_{65-x}Zr_{35}B_x$ (x=2.5, 5, 7.5, 10) alloy powders milled for 100 hours. The XRD pattern shows two broad peaks centered around 33^o and 44.5^o. This shows the formation of amorphous structure in the powders after prolonged milling. No crystalline peak appears in the XRD pattern of the as milled alloy powder after 100 hours of milling. It may however be noted that the primary XRD peaks of crystalline Fe and Zr appear at 33^o and 44.5^o, respectively. Also the possibility of recrystallization due to the heat generated inside the vials is less in the studied alloy powder due to the milling conditions used as has been mentioned earlier. In the early stages

[ξ] email : debabrata@iitg.ac.in

of milling, Fe rich solid solution is first formed with the dissolution of Zr in the Fe matrix with Boron particles embedded in the Fe-Zr interfaces [11]. As the milling progressed, partial amorphization starts occurring due to the structural reduction of Fe crystals. The defects and dislocations induced during the milling further deteriorate the crystalline structure progressively and ultimately lead to the formation of an amorphous powder.

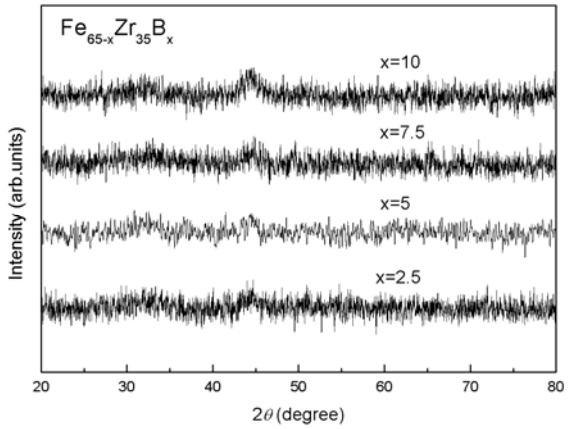

Figure 1. XRD pattern of $Fe_{65-x}Zr_{35}B_x$ (x=2.5, 5, 7.5, 10) of mechanically alloyed amorphous powders

In order to analyze the composition of the as-milled Fe-Zr powders and to evaluate possible contamination from the milling media, EDS analysis of the as-milled powders was carried out. It was seen that the composition after 100 hours of milling remains nearly the same as the nominal concentration. This confirms the homogeneity of the composition in the as-milled powders. The morphology of the alloy powder was studied by SEM. Figure 2 depicts the SEM micrograph of amorphous powders which show agglomerated particles after milling.

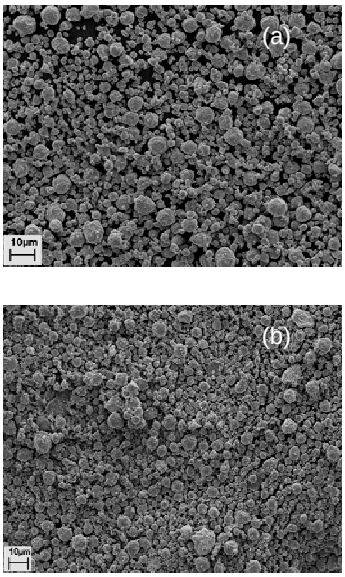

Figure 2: SEM micrographs of as-milled $Fe_{65-x}Zr_{35}B_x$ (x = 5(a), 10 (b)) alloy powders

Figure 3 shows the TEM image of the amorphous $Fe_{60}Zr_{35}B_5$ powder. Selected area electron diffraction (SAED) pattern has only diffused rings confirming the amorphous nature of the milled powder. Similar features have been observed for all other compositions studied in the present work.

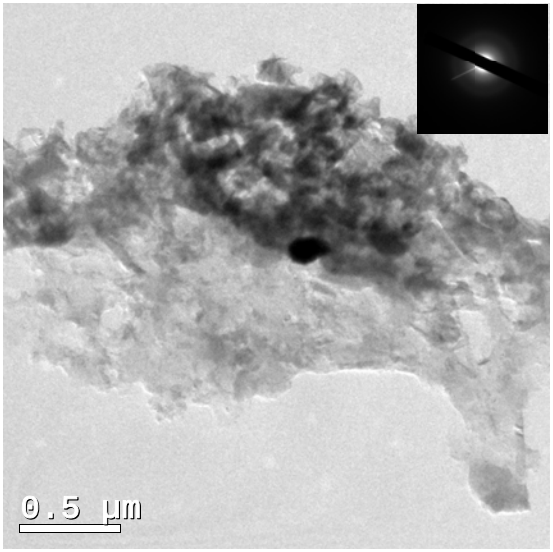

Figure 3. TEM bright field image of $Fe_{60}Zr_{35}B_5$ amorphous powder. Inset shows the SAED pattern with diffused rings

The crystallization behavior of the as-milled amorphous powder was studied using DSC. DSC curves of all the powder samples were recorded at constant heating rates (α) of 15, 20, 25 and 30 K/min. in the temperature range of 300 K to 970 K. Figure 4 shows the DSC curve of the as-milled amorphous alloy at a constant heating rate of 20 K/min. The relatively sharp and symmetric nature of exothermic peaks of the samples with boron content up to 7.5 at.% gives a qualitative confirmation of the homogeneity of these samples. However, the exothermic peak of the sample with 10 at.% B is asymmetric and broad unlike other samples. From the DSC curve it is clear that crystallization process starts at 800 K for sample with 2.5 at.% B and the crystallization temperature ($T_{cryst.}$) increases with the increase in the concentration of boron up to a critical concentration of boron (i.e., 7.5 at.%), and then decreases to a lower value for the 10 at.% B added sample. This sort of a behavior has also been observed in the case of ribbon samples of similar alloy system [12]. Addition of Boron makes it possible to achieve a denser packing and more intensive binding which leads to the slow atomic diffusion as result of which the crystallization temperature is enhanced. Table 1 shows the summary of the thermal behavior of the as milled amorphous Fe-Zr-B alloy. The enthalpy released during the exothermic process estimated from the area of the peak is listed in Table 1. Enthalpy increases with an increase in boron concentration. The activation energy of the alloy was calculated using Kissinger's relation shown in eq.(1) [13]

$$\ln \frac{T_{CRYS}^2}{\alpha} = \frac{E_A}{RT} + C \qquad (1)$$

where R is a universal gas constant and C is a constant. The calculated values of the activation energy E_A are listed in Table 1.

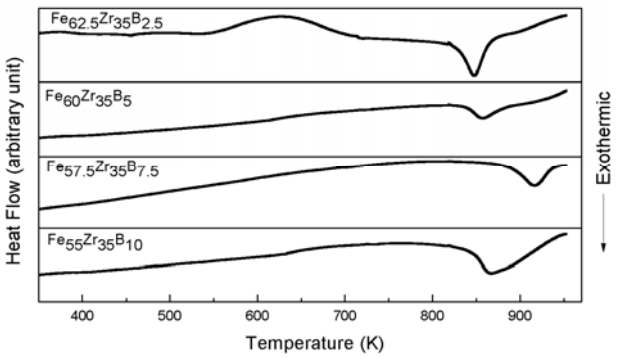

Figure 4. DSC curves of as-milled $Fe_{65-X}Zr_{35}B_x$ (x=2.5, 5, 7.5, and 10) alloy powders recorded at a constant heating rate of 20 K/min

Table 1. Crystallization summary of $Fe_{65-x}Zr_{35}B_x$ (x=2.5, 5, 7.5, 10) amorphous powder after DSC measurements

Composition	Crystallization Temperature T_{cryst} (K)	Enthalpy ΔH (J/g)	Activation Energy E_A (kJ/mol)
$Fe_{62.5}Zr_{35}B_{2.5}$	848	21	279±5
$Fe_{60}Zr_{35}B_5$	857	25	238±4
$Fe_{57.5}Zr_{35}B_{7.5}$	922	46	165±3
$Fe_{55}Zr_{35}B_{10}$	867	120	220±4

To investigate the magnetic properties of the as milled amorphous Fe-Zr-B alloy powder, room temperature magnetic measurements were carried out using VSM. The resulting coercivity and magnetization are shown in Fig. 5. The inset in the figure shows the hysteresis loop of the as-milled powders with different boron concentration. The coercivity (H_C) and saturation magnetization (M_S) show an increase up to the critical boron concentration of 7.5 at.%. This type of behavior is also seen in melt spun ribbons of similar alloy systems [14]. The increase in magnetization with the addition of boron is a result of an increase in the local magnetic moment of Fe with the addition of boron. The coercivity value obtained in the present studies is higher than that of melt quenched amorphous alloy of similar alloy systems [14]. The magnetic hardening observed in the present case may be due to domain wall pinning by the magnetic inhomogeneities such as fluctuations of the exchange energy, fluctuations of the local magnetic anisotropy, coupling of the elastic dipoles and atomic short range order clusters [15]. Synthesis route plays a decisive role in achieving good soft magnetic properties. Since MA adopted in the preparation of the present samples introduces the above mentioned inhomogeneity, magnetic hardening and hence a large coercivity is obtained in these powders. In order to investigate the possible reasons of magnetic hardening, the initial magnetization curve was fitted to the law of approach to saturation [15]

$$M = M_s\left(1 - \frac{a}{\sqrt{H}} - \frac{b}{H^2}\right) + \chi_p H \qquad (2)$$

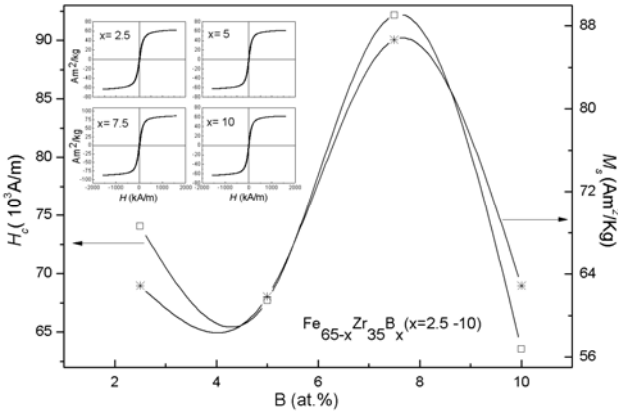

Figure 5. H_C and M_S values of $Fe_{65-x}Zr_{35}B_x$(x = 2.5, 5, 7.5, 10) amorphous alloy powders

where, M_S is saturation magnetization, H is applied field, χ_p is high field susceptibility originating from the increase in the number of spins which have the same direction in a domain, and a, b are constant coefficients. The coefficient b is related to the effective anisotropy. The $(a/\sqrt{H})$ term arises due to the local fluctuation of crystalline field (on a scale of few angstroms) in case of amorphous alloys [16] or small quasi dislocation loops [15] while the term b/H^2 is attributed to long range stresses induced by magnetoelastic interaction. Stresses accumulated in the powders can induce stress anisotropy *via* magnetoelastic coupling. The effective local anisotropy was calculated from the relation [17]

$$K_{eff} = \sqrt{\frac{15\, b\mu_0^2 M_S^2}{4}} \qquad (3)$$

The local anisotropy calculated using the above relation was found to be of the order of 10^5 J/m^3. The effective local anisotropy of the present sample is two orders higher than that of 3*d* based amorphous alloys (10^3 J/m^3). The higher value of the anisotropy gives rise to the higher coercivity. Magnetoelastic interaction as a result of magnetoelastic coupling between quasidislocation dipoles tends to dominate the hysteretic behavior of the mechanically alloyed amorphous alloys. Stress induced effective local anisotropy is the main factor behind the magnetic hardening in amorphous alloys, which needs to be reduced considerably for achieving good soft magnetic properties.

Conclusions

Amorphous $Fe_{65-x}Zr_{35}B_x$ (x = 2.5, 5, 7.5 and 10 at.%) powders were successfully synthesized by MA process. Structural characterization was done by XRD, SEM and TEM techniques to confirm the amorphous state and possible mechanisms of alloying. Crystallization temperature, enthalpy of crystallization and activation energy of crystallization showed anomaly at 7.5 at.%, indicating the presence of a critical composition in this amorphous system. Magnetic measurement of the alloy powder showed magnetic hardening in the amorphous alloy powders, which has been understood as due to the stress induced local anisotropy resulting from magneto-elastic coupling. This anisotropy has to be minimized for yielding better soft magnetic properties in these amorphous powders.

Acknowledgements

This work was financially supported by DAE-BRNS, India through a Young Scientist Research Award (2005/20/34/1/BRNS/ 376) for A.P. Permission from CIF, IIT Guwahati, India for the use of SEM, TEM (100/IFD/6278/2005-2006) and VSM (SR/S2/CMP-19/2006) is gratefully acknowledged.

References

1. F. B. Cantor and R.W. Cahn In: F.E. Luborsky, Editor, *Amorphous Metallic Alloys*, Butterworths Monographs in Materials (1983).
2. T. Kaneyoshi, *Introduction to Amorphous Magnet,* Worldscientific Singapore (1992).
3. C. Suryanarayana, *Prog. Mater. Sci.*, 46 (2000) 1.
4. R.B. Schwartz, C. K. Petrich, and C. K. Saw, *J. Non-cryst. Solids*, 76 (1985) 281.
5. L.Schultz, and E. Hellstern, *Appl. Phys. Lett.*, 48 (1986) 126.
6. J.S.Benjamin, *Sci. Amer.*, 234 (1976) 40.
7. L.M. Di, P. I. Loeff , and H. Bakker, S.S.A.R. Symp.Proc. *J. de Physique.* Vol. C4 (1993) p. 63.
8. L. Fernandez Barquın, J.C. Gomez Sal, P. Gorria, J.S. Garitaonandia, and J.M. Barandiaran., *J. Non-cryst. Solids*, 329 (1993) 94.
9. M. E. McHenry, M. A. Willard, and D. E. Laughlin, *Prog. Mater. Sci*, 44 (1999) 291.
10. C. Michaelsen and E. Hellstern, *J. Appl. Phys.*, 62 (1987) 117.
11. L. Schultz, *Mater. Sci. Eng.*, 97 (1988) 15.
12. T. Kemeny, D. Kaptas, L. F. Kiss, J. Balogh, I. Vincze, S. Szabo, and D. L. Beke, *Hyperfine Interact.*,130 (2000) 181.
13. H. E. Kissinger, *J. Res. Nat.Bur Std.*, 57 (1956) 217.
14. B.Yao, Y.Zhang, L. Si, H. Tan, and Y.Li, *J. Alloys. Comp.*, 370 (2004) 1.
15. H. Kronmueller, *IEEE Trans. Magn.*, 15 (1979) 1218.
16. R. Harris, M. Plischke, and M. J. Zuckermann, *Phys. Rev. Lett.*, 31 (1973) 160.
17. E. Loudghiri, A. Belayachi, N. Hassanain, O. Touraghe, A. Hassini, and H. Lassri, *Phys. Lett. A*, 371 (2007) 504.